

Received: 2019.12.31
Accepted: 2020.02.07
Available online: 2020.03.02
Published: 2020.04.28

Apoptosis Activation in Thyroid Cancer Cells by Jatrorrhizine-Platinum(II) Complex via Downregulation of PI3K/AKT/Mammalian Target of Rapamycin (mTOR) Pathway

Authors' Contribution:
Study Design A
Data Collection B
Statistical Analysis C
Data Interpretation D
Manuscript Preparation E
Literature Search F
Funds Collection G

BCD 1 **KeBin Lu**
BC 2,3 **Wenjun Wei**
BC 2,3 **Jiaqian Hu**
CDEF 2,3 **Duo Wen**
CD 2,3 **Ben Ma**
BC 2,3 **Wanlin Liu**
ACD 2,3 **Yu Wang**
AEF 2,3 **Zhongwu Lu**

1 Department of General Surgery, Yuyao People's Hospital of Zhejiang Province, Yuyao, Zhejiang, P.R. China
2 Department of Head and Neck Surgery, Fudan University Shanghai Cancer Center, Shanghai, P.R. China
3 Department of Oncology, Shanghai Medical College, Fudan University, Shanghai, P.R. China

Corresponding Authors: Zhongwu Lu, e-mail: zhwulu@163.com, Yu Wang, e-mail: yegfeqp@163.com
Source of support: Departmental sources

Background: Thyroid cancer, which is the most common endocrine cancer, has shown a drastic increase in incidence globally over the past decade. The present study investigated the thyroid cancer-inhibitory potential of jatrorrhizine-platinum(II) complex (JR-P(II)) *in vitro* and *in vivo*.

Material/Methods: The JR-P(II)-mediated cytotoxicity in thyroid carcinoma cells was determined by using MTT assay. Assessment of acetylated histones, tubulin, and DNA repair proteins was made by Western blot assays. Flow cytometry was used for apoptosis and ROS accumulation measurement.

Results: The JR-P(II) suppressed proliferative capacity of SW1736, BHP7-13, and 8305C cells. JR-P(II) treatment markedly promoted expression of acetylated histone H3, H4, and tubulin in a dose-dependent manner. Treatment with JR-P(II) significantly elevated the proportion of cells in sub-G1 and promoted cleaved caspase-3 and -9. In JR-P(II)-treated cells, DCFH-DA fluorescence was much higher relative to control cells. The JR-P(II) treatment consistently suppressed expression of pS6, p-ERK1/2, p-4E-BP1, and p-AKT, and increased p-H2AX expression and suppressed KU70 and KU80 protein levels. The level of RAD51 was repressed in JR-P(II)-treated cells. JR-P(II) administration in mice caused no significant change in body weight, and it inhibited SW1736 tumor growth in mice.

Conclusions: The JR-P(II) induced cytotoxicity in thyroid cancer cells by inhibiting the mechanism responsible for repair of double-stranded DNA. The *in vivo* data also revealed that JR-P(II) effectively inhibits thyroid tumor growth by inducing DNA damage. Thus, our results suggest that further evaluation of JR-P(II) as a therapeutic candidate for thyroid cancer is warranted.

MeSH Keywords: **Antibody-Dependent Cell Cytotoxicity • Apoptosis • Chromosomal Proteins, Non-Histone • Parathyroid Neoplasms**

Full-text PDF: <https://www.medscimonit.com/abstract/index/idArt/922518>

 2576  —  9  30



Background

Thyroid cancer, a commonly diagnosed endocrine malignancy, has shown a drastic increase in incidence globally over the past decade [1]. Although increased incidence of thyroid cancer reveals a 50% increase in small tumors, its etiology is unknown [2,3]. Histologically, there are 3 types of thyroid cancer, depending on origin: anaplastic, papillary, and follicular [4]. Of these 3 types, anaplastic thyroid carcinoma has the highest fatality rate, with median survival of less than 6 months. Well-differentiated thyroid carcinoma, including papillary and follicular cancer, is detected in around 90% of patients with thyroid malignancy. The average survival of patients with well-differentiated thyroid carcinoma is increased to 10 years by the treatment combination of radioactive iodine, thyroid hormone suppression, and surgical resection [5]. However, progression to metastatic stage reduces survival of patients with well-differentiated thyroid carcinoma to 3–5 years [5].

Unrestricted proliferation, escape from apoptosis, and rapid cell cycle progression are hallmarks of cells in malignant tumors, sometimes driven by histone deacetylases (HDACs), which deacetylate the lysine residues of histones and non-histones involved in transcription, thereby affecting apoptosis and proliferation [6,7]. HDACs are very important molecular targets for development of cancer therapies [6,7]. Malignant tumor cells are more sensitive to the cytotoxicity of HDAC inhibitors than are benign cells [6]. Inhibitors of HDACs, which are generally low-molecular-weight molecules, induce ROS accumulation and damage DNA, activate apoptosis, and finally exhibit cytotoxicity in carcinoma cells [6]. In relation to normal tissues of the thyroid gland, HDAC1 and 2 have highest overexpression in ATC. Papillary carcinoma cells also show higher levels of HDAC1 and 2, suggesting involvement of these HDACs in the tumorigenicity of thyroid cancer [8,9]. The inhibitors of HDACs initiate re-differentiation of cells and activate apoptosis in thyroid carcinoma cells [10]. This highlights the potential of HDAC inhibitors for thyroid cancer therapy via apoptosis induction and cellular re-differentiation.

Cisplatin and other related complexes like oxaliplatin and carboplatin used to treat tumors induce several adverse effects [11,12]. To eliminate these adverse effects, various other complexes of platinum have been synthesized and evaluated for carcinoma therapy [11,13]. Moreover, many natural products have been linked to metals and the corresponding metal-complexes investigated for treatment of cancer [14,15]. Recently, Jatrorrhizine, obtained from *Tinospora capillipes Gagnep*, has been shown to possess anti-tumor potential and other activities [16,17]. The complexes of jatrorrhizine with Pt(II) metal were synthesized and exhibited anti-cancer activity. The present study evaluated jatrorrhizine-platinum(II) complex (JR-P(II)) for anti-tumor potential against thyroid cancer.

Material and Methods

Cell lines and culture

The SW1736, BHP7-13, and 8305C cell lines were provided by the Cell Bank of the Chinese Academy of Sciences (Shanghai, China). The cell lines obtained were maintained in RPMI 1640 medium containing NaHCO_3 (2.2 g/L). The medium also contained FCS (10%), penicillin (100,000 units/L), and streptomycin (100 mg/L). The cell lines were maintained in an incubator under conditions of 37°C temperature and 5% CO_2 humid atmosphere.

Cell proliferation analysis

The SW1736, BHP7-13, and 8305C cells were put in 96-well plates at 1×10^5 cells per well concentration and cultured for 24 h. Afterwards, cells were treated with 1.5, 3.0, 6.0, 12.0, 24.0, and 48 μM concentrations of JR-P(II) for 24 and 48 h. Then, 20 μl volume of MTT solution (5 mg/ml) was put into each well of the plate and cell incubation was performed for 4 h. Then, medium was decanted and 150 μl DMSO was added to the wells for dissolution of formazan formed from MTT. The plates were shaken for 20 min, followed by immediate optical density recording at 485 nm using a spectrophotometer to measure viability.

Western blot assay

The SW1736 and BHP7-13 cells treated with 1.5, 6.0, and 24.0 μM of JR-P(II) for 48 h were collected and then lysed using lysis buffer. The buffer contained Tris-HCl (40 mM; pH 7.4), sodium chloride (150 mM), and Triton X-100 (1% v/v), along with the protease inhibitors. Lysate centrifugation for 20 min at 12 000 g at 4°C was followed by determination of protein concentration in supernatant using a bicinchoninic acid protein kit. The protein samples (30 μg per lane) were subjected to resolution by electrophoresis on 10% SDS-PAGE followed by transfer to PVDF membranes. The membrane blocking on incubation with 5% skimmed milk in TBS plus Tween-20 (0.1%) was carried out for 2 h at room temperature. The samples were subjected to probing on incubation with primary antibodies anti-caspase-3, anti-p-AKT, anti-p-ERK1/2, anti-p-S6, anti-p-H2AX, anti-KU70, anti-KU80, anti-p-4E-BP1, anti-RAD52, anti-ERCC1 anti-PCNA, and α -tubulin primary antibodies (Cell Signaling) overnight at 4°C. Then, 1X PBST washing of membranes was followed by incubation for 2 h with horseradish peroxidase-conjugated secondary antibody. The immunoblots were visualized using SignalFire™ Plus ECL Reagent and quantified using Image J version 2.0 software.

Analysis of apoptosis

The apoptosis induction by JR-P(II) in SW1736 and BHP7-13 cells was assessed by evaluation of cells in sub-G1 phase. Briefly, the cells at 1×10^6 cells per well concentration were put in 6-well plates containing 2 mL media and treated for 48 h with 1.5, 6.0, and 24.0 μM JR-P(II). The adherent cells were PBS washed 2 times, fixed in 70% ethyl alcohol, and subsequently incubated for 20 min with RNase A and 5 $\mu\text{g}/\text{mL}$ solution of propidium iodide at 37°C. Cytometry (BD FACSCalibur) was performed to assess DNA content of the cells for detection of sub-G1 cell count.

Analysis of ROS accumulation

The SW1736 and BHP7-13 cells at a concentration of 1×10^6 cells per well were put in 6-well plates containing 2 mL media and treated for 48 h with 1.5, 6.0, and 24.0 μM JR-P(II). The adherent cells were collected after trypsinization, followed by incubation for 40 min with DCFH-DA (10 $\mu\text{mol}/\text{L}$) in the dark at 37°C. After centrifugation, cells were re-suspended in PBS and then probed for DCFH-DA fluorescence measurement by flow cytometry (BD FACSCalibur).

Mice

Thirty female nude mice (6 weeks old) were obtained from the Experimental Animal Centre of the Zhejiang University (Hangzhou, China). The mice were housed individually in sterile conditions in cages in the animal house and were exposed to a 12-h light/dark cycle. The temperature was maintained at $23 \pm 2^\circ\text{C}$ and humidity 65%. The study was approved by the Animal Ethics Committee, Hospital of Fudan University, Shanghai Medical College, Fudan University, Shanghai 200032, China (approval no. Su/2016/045). All the experimental protocols were performed in accordance with the guidelines issued by the National Institute of Health, China.

Establishment of thyroid tumor xenograft and treatment

The mice were randomly assigned into 3 groups of 10 each: normal control, untreated, and JR-P(II) treatment. The mice in the untreated and JR-P(II) treatment groups were intraperitoneally injected with ketamine hydrochloride plus xylazine hydrochloride anesthesia. SW1736 cells (2×10^6) in 100 μL PBS were injected subcutaneously into the flanks of mice. Mice in the treatment group were intraperitoneally injected with 24 mg/kg of JR-P(II) daily for 14 days. Mice in the normal and untreated groups received equal volumes of normal saline. Changes in body weight were measured on alternate days and tumor volumes were recorded using electronic calipers. Five mice from each group were sacrificed using carbon dioxide on day 7 and 5 on day 14 of treatment to excise the tumors.

The tumors were treated with protein extraction buffer, homogenized, and sonicated on ice. The tissue lysate was centrifuged to collect the supernatants, which were stored in liquid nitrogen until further analysis. The expression of proteins was measured by Western blotting. Body weights of mice were recorded on alternate days during 14 days (on days 2, 4, 6, 8, 10, 12, and 14 of the treatment), and the tumor weights were measured on days 7 and 14.

Statistical analysis

The data are expressed as mean \pm standard deviations of triplicate experiments. Analysis of the data was performed using SPSS version 17.0 software (SPSS, Inc., Chicago, IL, USA). The differences were determined by one-way analysis of variance (ANOVA) and *t* test. $P < 0.05$ was regarded as indicating statistically significant differences.

Results

JR-P(II) inhibits thyroid cancer cell proliferation

Proliferation of SW1736, BHP7-13, and 8305C cells following JR-P(II) treatment was measured at 24 and 48 h (Figure 1). The JR-P(II) at 1.5, 3.0, 6.0, 12.0, 24.0, and 48 μM concentrations suppressed proliferative capacity of the cells in a concentration- and time-dependent manner. Treatment with JR-P(II) at 1.5 $\mu\text{mol}/\text{L}$ for 24 h reduced SW1736, BHP7-13, and 8305C cell proliferation by 12%, 15%, and 17%, respectively. The JR-P(II) treatment at 24.0 μM for 24 h reduced SW1736, BHP7-13, and 8305C cell proliferation by 55%, 59%, and 64%, respectively. Proliferation rates of SW1736, BHP7-13, and 8305C cells were suppressed by 21%, 26%, and 29%, respectively, by treatment with 1.5 μM JR-P(II) at 48 h. The SW1736, BHP7-13, and 8305C cell proliferation was suppressed by 77%, 79%, and 82%, respectively, by treatment with 24.0 μM JR-P(II).

JR-P(II) promotes histones H3, histone H4, and tubulin acetylation

Effect of JR-P(II) on histone and tubulin acetylation was evaluated at 1.5, 6.0, and 24.0 μM in SW1736 and BHP7-13 cells (Figure 2). The JR-P(II) treatment significantly increased expression of acetylated histone H3, H4, and tubulin in a concentration-dependent manner at 48 h relative to control cells. The increase in acetylated histone H3, H4, and tubulin level in SW1736 and BHP7-13 cells was evident from 1.5 μM . The upregulation of acetylated histone H3, H4, and tubulin by JR-P(II) in SW1736 and BHP7-13 cells was strongest at 24.0 μM concentration.

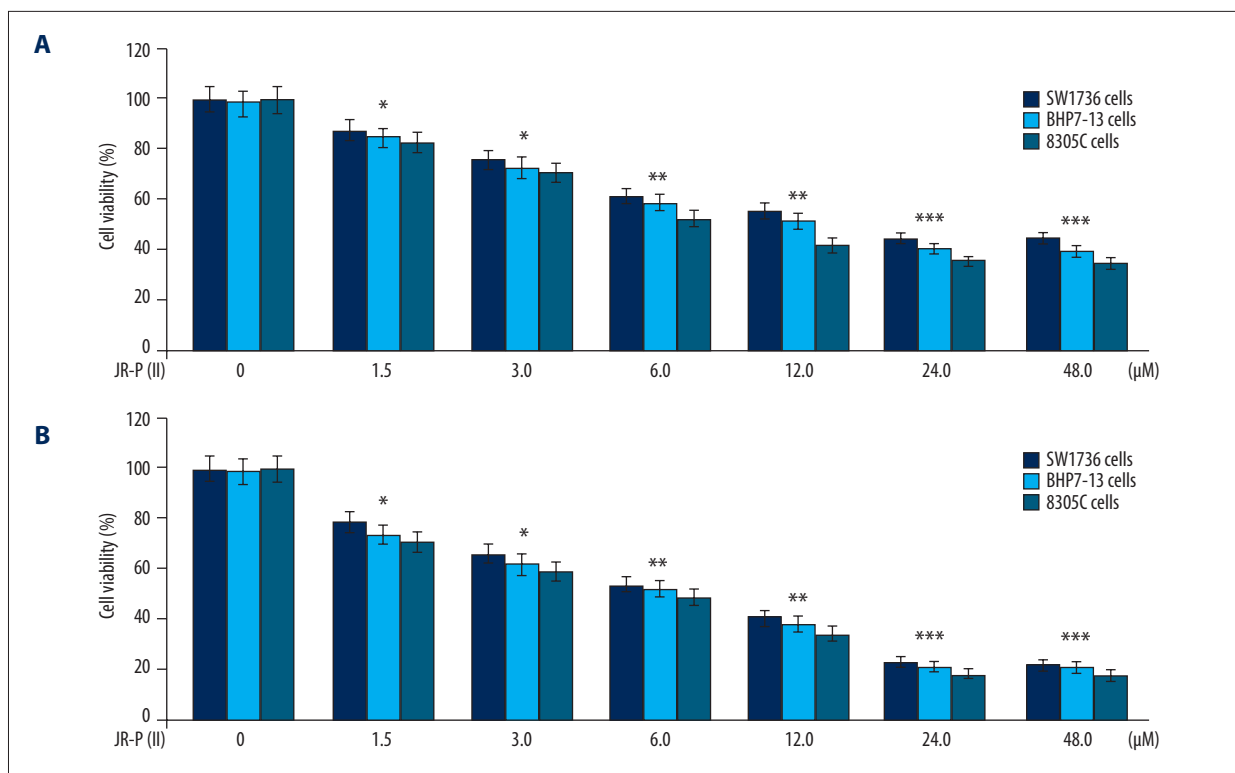


Figure 1. JR-P(II) induces cytotoxicity in SW1736, BHP7-13, and 8305C cells. **(A)** Effect of JR-P(II) at 1.5, 3.0, 6.0, 12.0, 24.0, and 48 μM concentrations was measured by MTT assay following 24 h of incubation. **(B)** The proliferative potential of cells was measured at 48 h after JR-P(II) treatment. * P<0.05, ** P<0.02 and *** P<0.01 vs. cells exposed to DMSO.

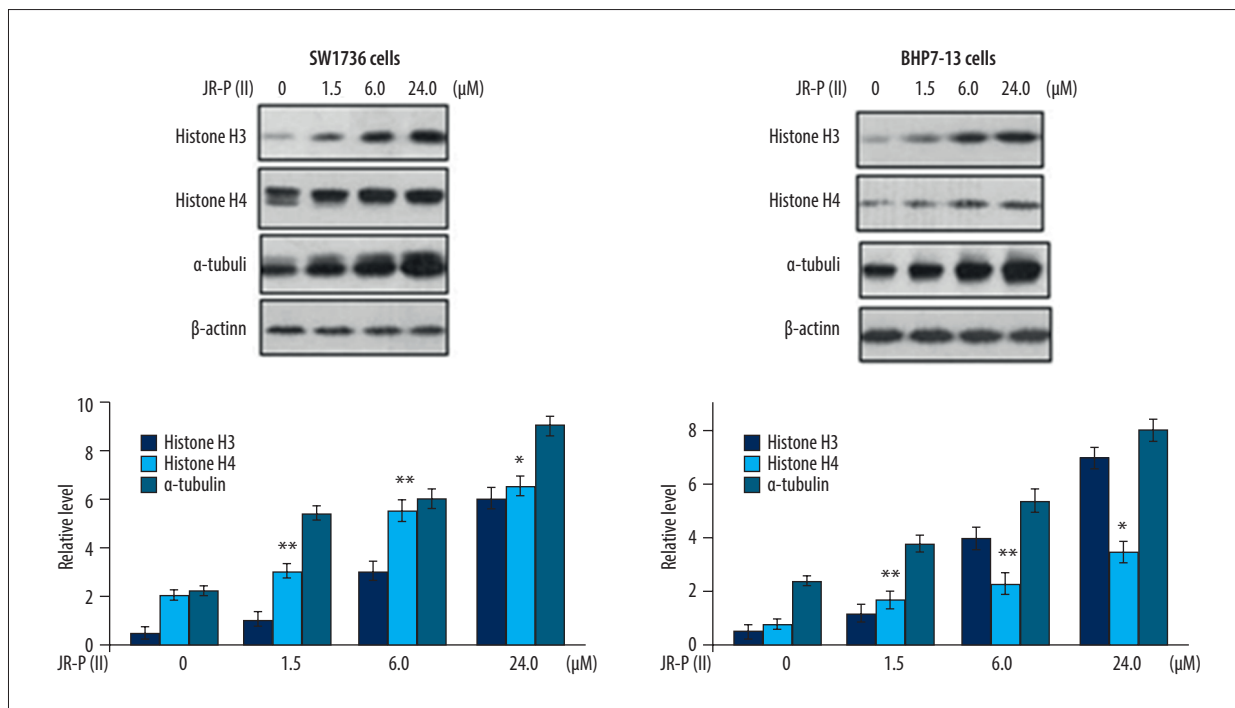


Figure 2. Effect of JR-P(II) on level of acetylated histone H3, H4, and tubulin in SW1736 and BHP7-13 cells. The JR-P(II) at 1.5, 6.0, and 24.0 μM was mixed in DMEM medium, and cells were incubated for 48 h in it. The acetylated histone and tubulin levels were evaluated by Western blot assay. * P<0.05 and ** P<0.02 vs. cells exposed to DMSO.

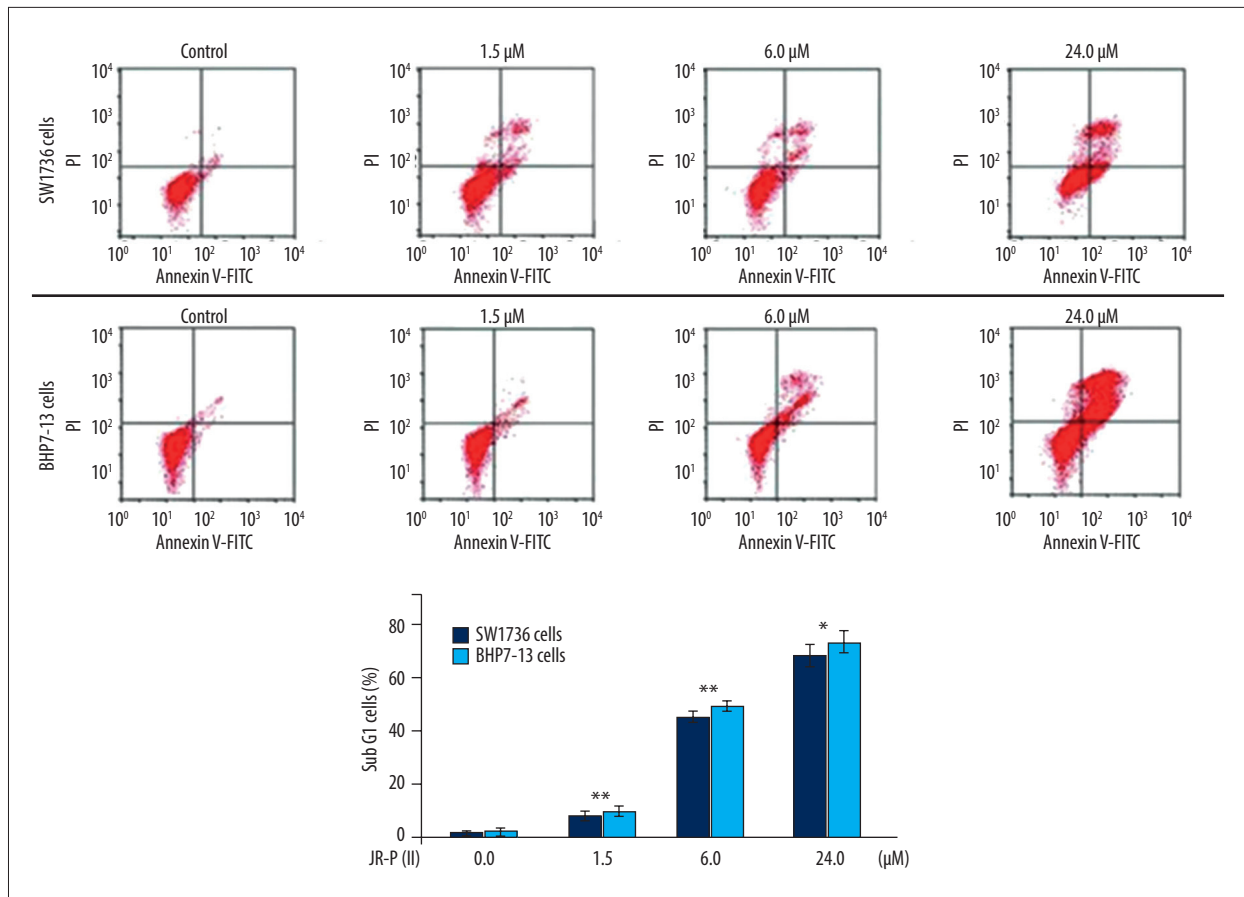


Figure 3. Effect of JR-P(II) on apoptosis in SW1736 and BHP7-13 cells. The DNA content of JR-P(II) treated cells was measured at 48 h by flow cytometry. In SW1736 and BHP7-13 cells JR-P(II) treatment at 1.5, 6.0, and 24.0 μM for 48 h was followed by flow cytometry. * P<0.05 and ** P<0.02 vs. cells exposed to DMSO.

JR-P(II) mediates apoptosis in SW1736 and BHP7-13 cells

Apoptosis induction by JR-P(II) at 1.5, 6.0, and 24.0 μM in SW1736 and BHP7-13 cells was assessed by evaluation of cells in sub-G1 phase (Figure 3). The JR-P(II) treatment significantly increased the proportion of SW1736 and BHP7-13 cells in sub-G1 relative to the control. The increase in sub-G1 cells caused by JR-P(II) was significant from 1.5 μM in SW1736 and BHP7-13 cells. The data from flow cytometry also confirmed JR-P(II) induced apoptosis in SW1736 and BHP7-13 cells.

JR-P(II) mediated caspase-3 activation in SW1736 and BHP7-13 cells

The confirmation of apoptosis induction by JR-P(II) in SW1736 and BHP7-13 cells was made by evaluation of caspase-3 activation (Figure 4). JR-P(II) significantly increased the levels of cleaved caspase-3 in SW1736 and BHP7-13 cells from 1.5 μM. The cleavage of cleaved caspase-3 by JR-P(II) was maximum at 24 μM.

JR-P(II) mediated ROS accumulation in thyroid cancer cells

The ROS accumulation by JR-P(II) in SW1736 and BHP7-13 cells was evaluated at 1.25, 6.0, and 12.0 μM using DCFH-DA (Figure 5A). In JR-P(II)-treated SW1736 and BHP7-13 cells, DCFH-DA fluorescence was much higher relative to control cells. In SW1736 cells, DCFH-DA fluorescence increased to 183.4±4.5 (P<0.001) after treatment with 6.0 μM JR-P(II) compared to 78.2±2.1 in control (Figure 5B). The DCFH-DA fluorescence in BHP7-13 cells increased to 198.5±5.0 after treatment with 12.0 μM JR-P(II) compared to 84.3±3.2 in control (P<0.001).

JR-P(II) inhibited PI3K/AKT/mTOR signaling pathway in thyroid cancer cells

In SW1736 and BHP7-13 cells, expression of pS6, p-ERK1/2, p-4E-BP1, and p-AKT was assessed following treatment with JR-P(II) at 1.25, 6.0, and 12.0 μM (Figure 6). The JR-P(II) treatment consistently suppressed expression of pS6, p-ERK1/2, p-4E-BP1, and p-AKT in SW1736 and BHP7-13 cells. The repression of pS6, p-ERK1/2, p-4E-BP1, and p-AKT in SW1736

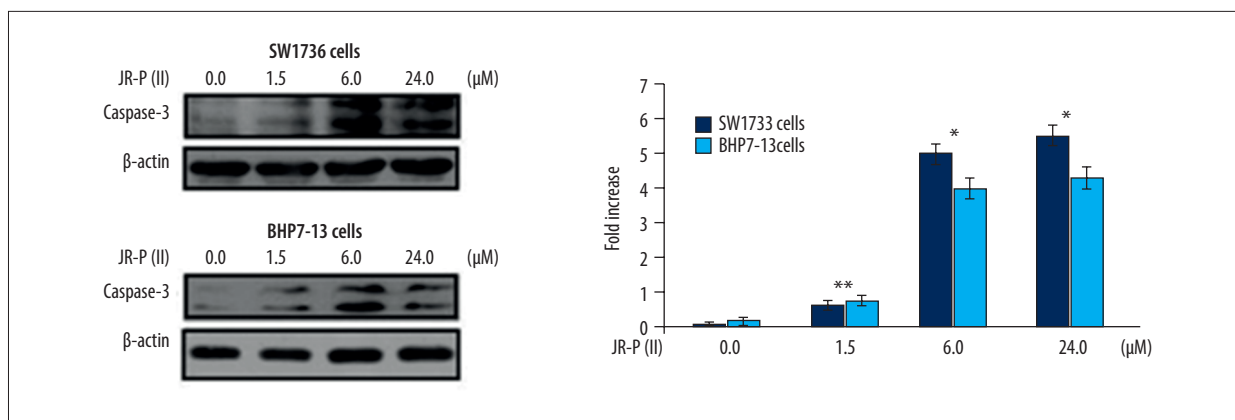


Figure 4. Effect of JR-P(II) on cleaved caspase-3 in SW1736 and BHP7-13 cells. In SW1736 and BHP7-13 cells JR-P(II) treatment at 1.5, 6.0, and 24.0 μM for 48 h was followed by assessment of caspase-3 cleavage. * $P<0.05$ and ** $P<0.02$ vs. cells exposed to DMSO.

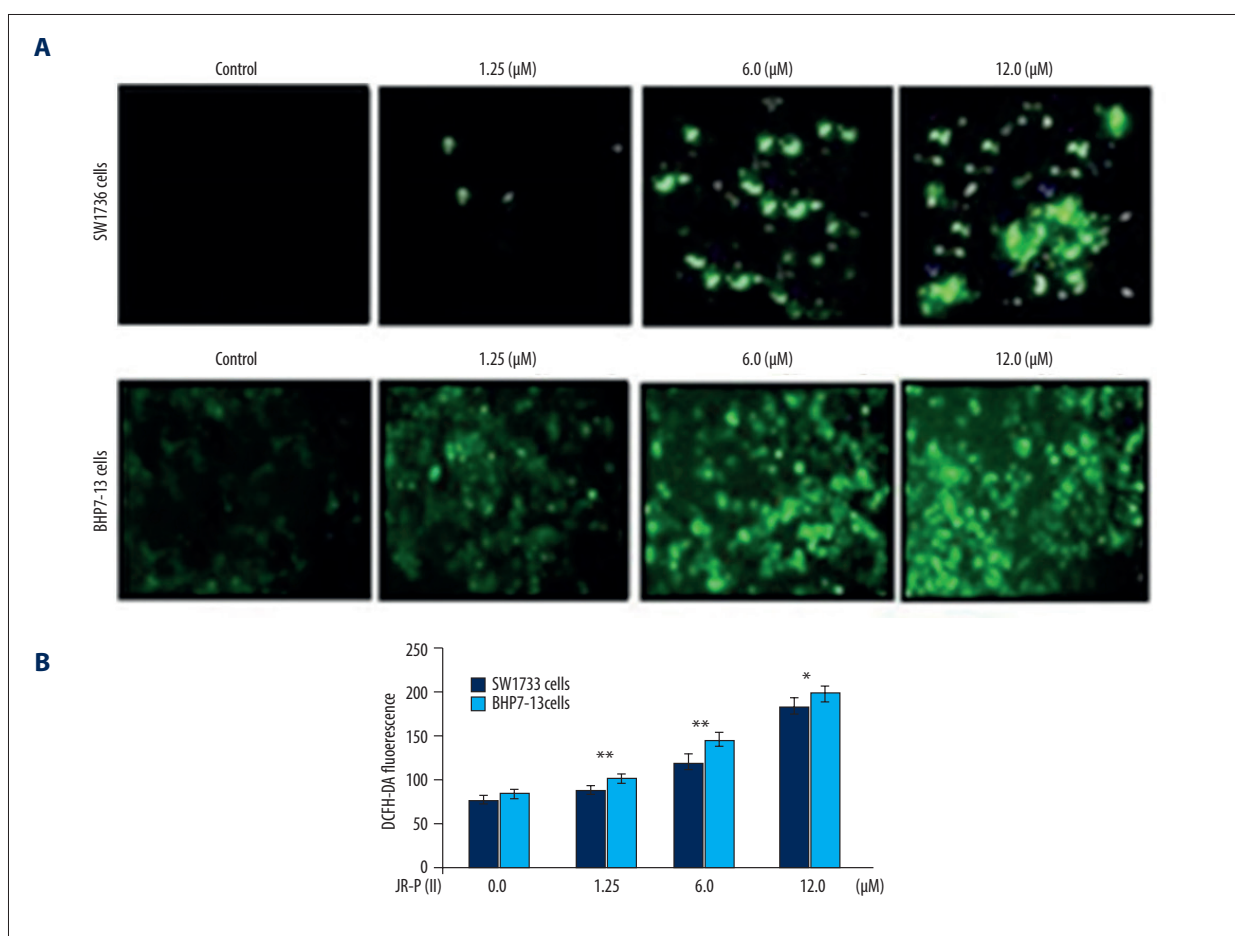


Figure 5. (A, B) Effect of JR-P(II) on accumulation of ROS in SW1736 and BHP7-13 cells. The cells after JR-P(II) treatment at 1.25, 6.0, and 12.0 μM were evaluated for DCFH-DA fluorescence by flow cytometry. * $P<0.05$ and ** $P<0.02$ vs. cells exposed to DMSO.

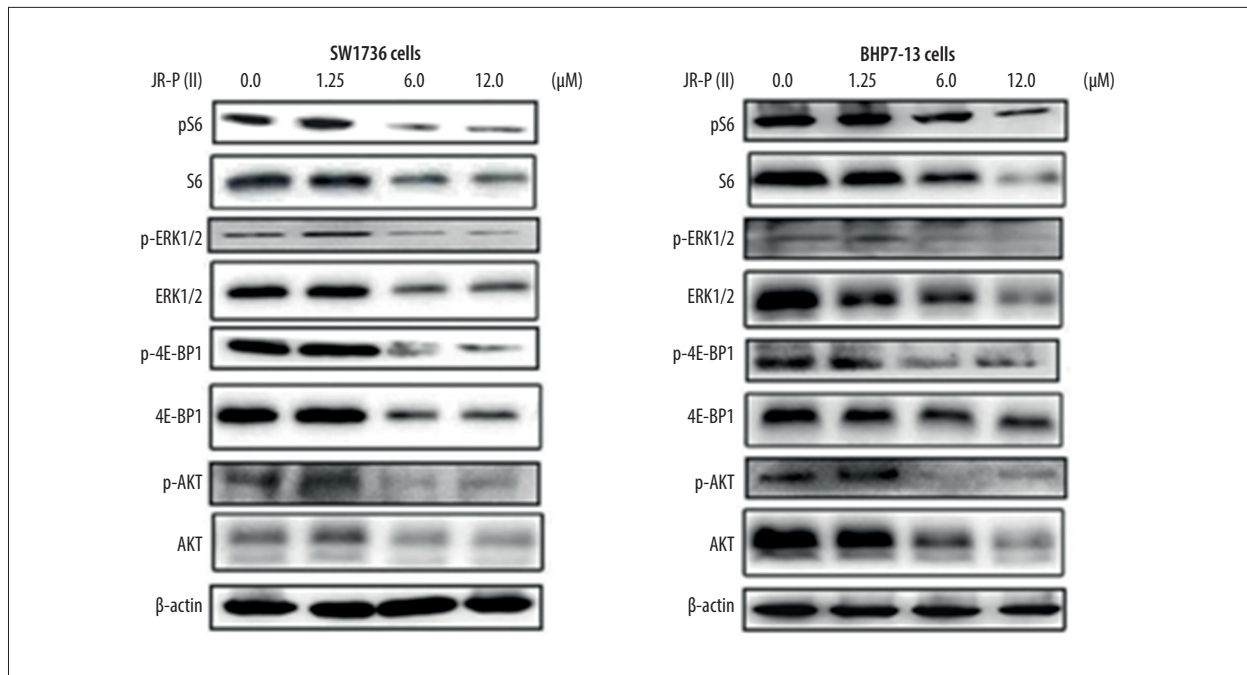


Figure 6. Effect of JR-P(II) on PI3K/AKT/mTOR signaling proteins. The SW1736 and BHP7-13 cells were treated with 1.25, 6.0, and 12.0 μM JR-P(II). Immunoblotting was used for evaluation of pS6, p-ERK1/2, p-4E-BP1, and p-AKT protein expression.

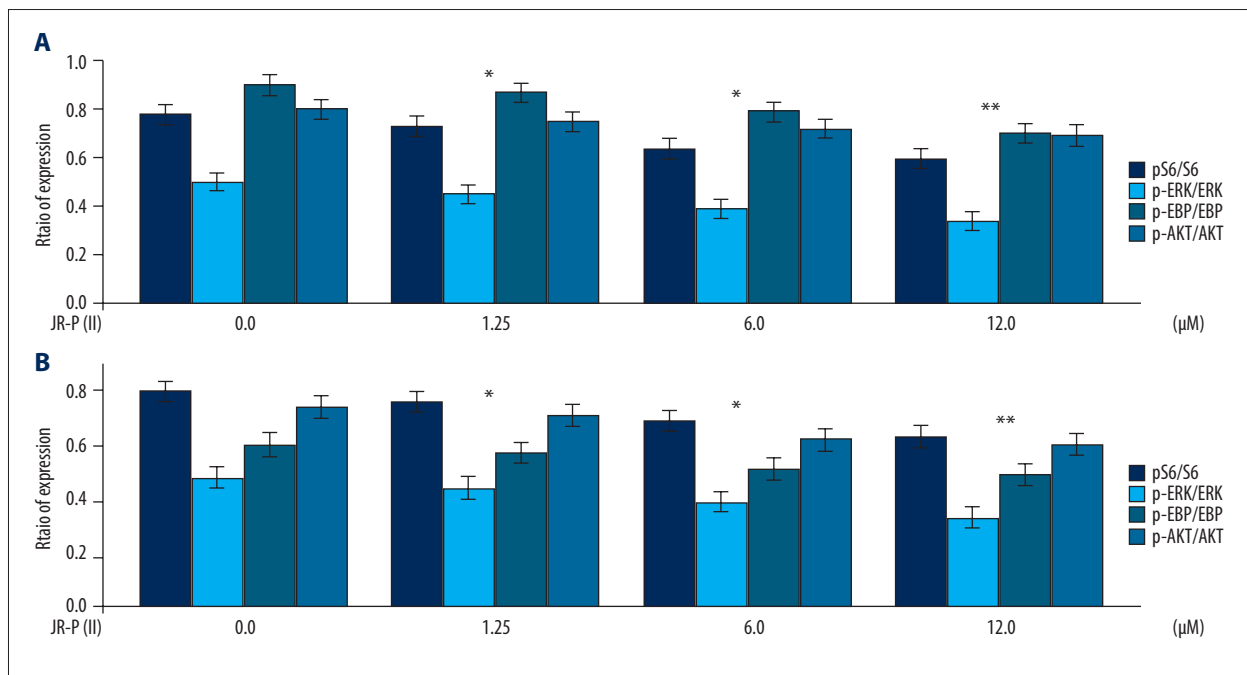


Figure 7. Effect of JR-P(II) on PI3K/AKT/mTOR signaling proteins. The SW1736 (A) and BHP7-13 (B) cells were treated with 1.25, 6.0, and 12.0 μM JR-P(II). Densitometry analysis of the Western blotting data for pS6/S6, p-ERK1/2/ERK1/2, p-4E-BP1/4E-BP1, and p-AKT/AKT in SW1736 and BHP7-13 cells.

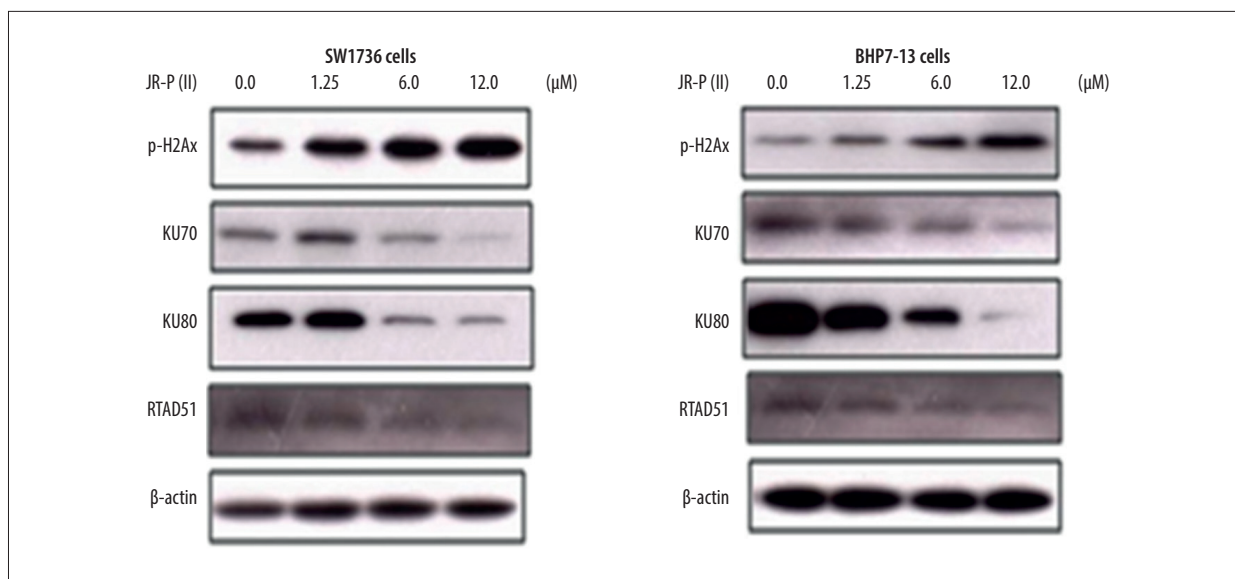


Figure 8. Effect of JR-P(II) on DNA repair and damage proteins. The SW1736 and BHP7-13 cells were treated with 1.25, 6.0, and 12.0 μM JR-P(II). Immunoblotting was used for evaluation of KU70, ERCC1, KU80, and RAD51 protein expression.

and BHP7-13 cells by JR-P(II) was found to be concentration-dependent. The densitometry analysis showed decreases in the ratios of pS6/S6, p-ERK1/2/ERK1/2, p-4E-BP1/4E-BP1, and p-AKT/AKT in SW1736 and BHP7-13 cells after treatment with JR-P(II), and the effect was concentration-dependent (Figure 7).

JR-P(II) promoted DNA damage in thyroid cancer cells

The immunoblotting was performed for evaluation of changes in DNA damage protein expression by JR-P(II) at 48 h (Figure 8). The JR-P(II) treatment of SW1736 and BHP7-13 cells at 1.25, 6.0, and 12.0 μM significantly elevated p-H2AX expression. The KU70 and KU80 repair protein level was suppressed significantly by JR-P(II) treatment in SW1736 and BHP7-13 cells. The level of the HR repair protein RAD51 was also repressed in SW1736 and BHP7-13 cells after treatment with JR-P(II).

JR-P(II) inhibited tumor growth in murine model

The effect of JR-P(II) on SW1736 tumor growth was evaluated *in vivo* in athymic nude mice (Figure 9). The mice bearing established flank tumors were intraperitoneally injected with 24-mg/kg doses of JR-P(II) daily for 14 days. The JR-P(II) administration in mice caused no significant change in body weight (Figure 9A). The SW1736 tumor growth in mice was significantly suppressed ($P < 0.015$) by treatment with 24-mg/kg doses of JR-P(II) (Figure 9B). In JR-P(II)-treated mice, tumor tissues expression of pH2AX and acetylated histone H3 and H4 were increased compared to controls (Figure 9C). The level of cleaved caspase-3 was increased in the tumor tissues of JR-P(II)-treated mice.

Discussion

The present study demonstrates that JR-P(II) inhibits SW1736, BHP7-13, and 8305C cell proliferation and promotes acetylation of histones. The acetylation of histone H3, histone H4, and tubulin is promoted by the inhibitors of HDAC. It is reported that accumulation of ROS and activation of apoptosis is enhanced in transformed cells by the HDAC inhibitors [6,18]. In the present study, JR-P(II) treatment significantly increased accumulation of ROS in SW1736 and BHP7-13 cells. These findings were consistent with the mechanism by which HDAC inhibitors affect malignant tumor cells. The proliferation and survival of thyroid carcinoma cells is mainly regulated by 2 signaling pathways: PI3K/AKT/mTOR and RAS/RAF/ERK [19]. Some of the thyroid malignancy treatment strategies use these pathways as the molecular targets [20,21]. Breaks in the double-stranded structure of DNA are considered to be serious DNA damage, characterized by upregulation of p-H2AX [22]. In the present study, JR-P(II) treatment inhibited phosphorylation of AKT in SW1736 and BHP7-13 cells in a concentration-dependent manner. The data showed increased levels of p-H2AX in SW1736 and BHP7-13 cells after treatment with JR-P(II). This indicated formation of double-stranded breaks in DNA as the mechanism of cytotoxicity induced by JR-P(II) in SW1736 and BHP7-13 cells.

The breaks in DNA are repaired by the expression of non-homologous end joining (NHEJ) repairing proteins (KU70 and KU80) and homologous recombination proteins such as RAD51 [23]. The KU70 and KU80 proteins, after recognizing the DNA breaks, activate DNA kinases, which immediately repair the damage [23,24]. The RAD51 protein repairs DNA breaks

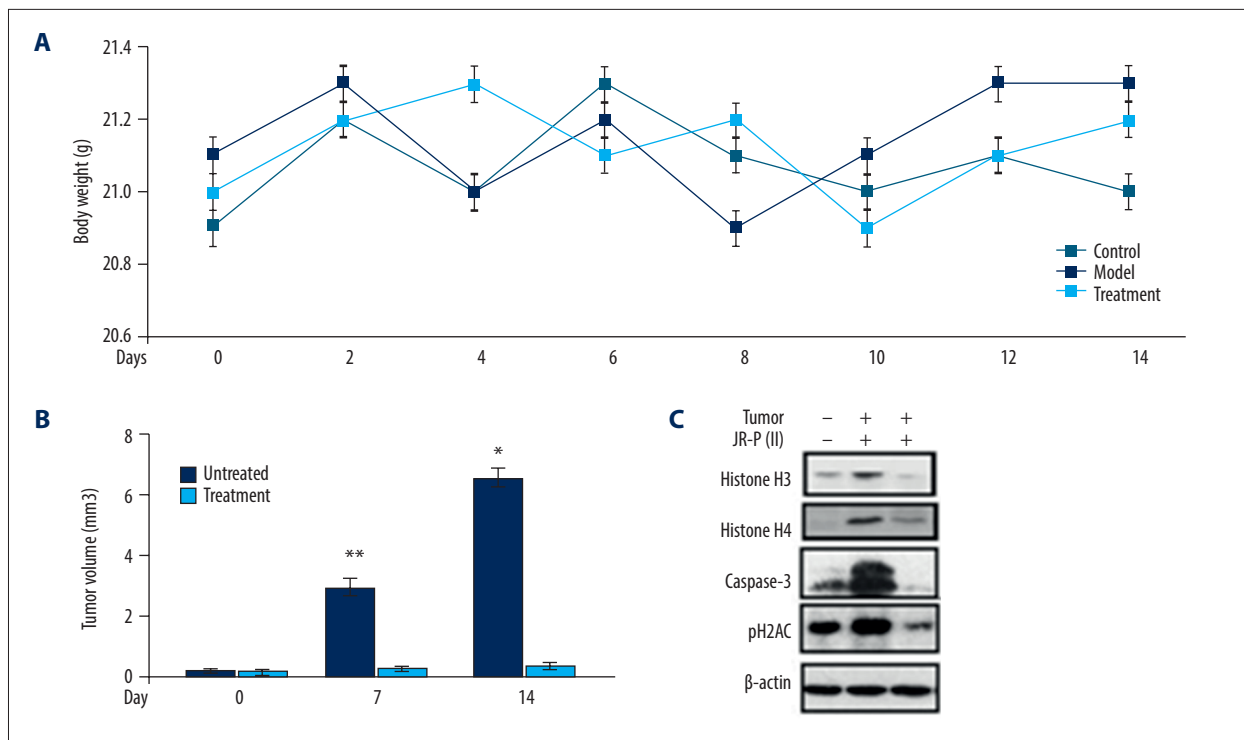


Figure 9. Effect of JR-P(II) on tumor growth *in vivo*. The mice bearing established flank tumors were treated by intraperitoneal injection of 24 mg/kg of JR-P(II) daily for 14 days. **(A)** Body weight of mice was recorded on alternate days during the 14 days of the study (days 2, 4, 6, 8, 10, 12, and 14 of treatment). **(B)** The tumor weight was measured on days 7 and 14 of the study. **(C)** The acetylated protein levels and cleaved caspase-3 expression in tumors were evaluated on day 14 by immunoblot assay. * $P < 0.05$ and ** $P < 0.02$ vs. control.

by binding to single DNA strands at the resected end, thereby catalyzing the synthesis [25]. Studies have demonstrated that targeting RAD51 leads to development of very important defects [25,26]. In the absence of NHEJ proteins, an alternate pathway known as the SSA pathway plays a role in repairing the DNA breaks [23,27]. However, it has been found that overexpression of p-H2AX makes the SSA pathway unable to repair DNA breaks [28]. The expression of DNA repair proteins is suppressed by many HDAC inhibitors, resulting in cell damage and apoptosis [29]. The HDACs like HDAC1 and HDAC2 prevent DNA damage by increasing NHEJ expression, while HDAC 9 and HDAC10 enhance the level of homologous recombination proteins [30]. In the present study, DNA repair was inhibited and DNA damage was promoted by JR-P(II) in SW1736 and BHP7-13 cells. The JR-P(II) treatment significantly elevated p-H2AX expression and suppressed KU70, KU80, and

AD51 level in SW1736 and BHP7-13 cells. The JR-P(II) treatment of mice bearing SW1736 tumor xenografts inhibited tumor growth without inducing any adverse effects. The levels of p-H2AX and acetylated histone H3 and H4 were also increased significantly by JR-P(II) in the mouse model of thyroid cancer.

Conclusions

JR-P(II) induced cytotoxicity in thyroid cancer cells by inhibiting the mechanism responsible for repair of double-stranded DNA. The *in vivo* data also revealed that JR-P(II) effectively inhibits thyroid tumor growth by inducing DNA damage without influencing body weights of mice. Our data suggest that further evaluation of JR-P(II) as a therapeutic candidate for thyroid cancer is warranted.

References:

- Ito Y, Nikiforov YE, Schlumberger M, Vigneri R: Increasing incidence of thyroid cancer: Controversies explored. *Nat Rev Endocrinol*, 2013; 9: 178–84
- Davies L, Welch HG: Increasing incidence of thyroid cancer in the United States, 1973–2002. *JAMA*, 2006; 295: 2164–67
- Cramer JD, Fu P, Harth KC et al: Analysis of the rising incidence of thyroid cancer using the Surveillance, Epidemiology and End Results national cancer data registry. *Surgery*, 2010; 148: 1147–53; discussion: 1152–53
- Xing M: Molecular pathogenesis and mechanisms of thyroid cancer. *Nat Rev Cancer*, 2013; 13: 184–99
- Haugen BR, Alexander EK, Bible KC et al: 2015 American Thyroid Association management guidelines for adult patients with thyroid nodules and differentiated thyroid cancer: The American Thyroid Association guidelines task force on thyroid nodules and differentiated thyroid cancer. *Thyroid*, 2016; 26: 1–133
- Marks PA: Histone deacetylase inhibitors: A chemical genetics approach to understanding cellular functions. *Biochim Biophys Acta*, 2010; 1799: 717–25
- Minucci S, Pelicci PG: Histone deacetylase inhibitors and the promise of epigenetic (and more) treatments for cancer. *Nat Rev Cancer*, 2006; 6: 38–51
- Borbone E, Berlingieri MT, De Bellis F et al: Histone deacetylase inhibitors induce thyroid cancer-specific apoptosis through proteasome-dependent inhibition of TRAIL degradation. *Oncogene*, 2010; 29: 105–16
- Furuya F, Shimura H, Suzuki H et al: Histone deacetylase inhibitors restore radioiodide uptake and retention in poorly differentiated and anaplastic thyroid cancer cells by expression of the sodium/iodide symporter thyroperoxidase and thyroglobulin. *Endocrinology*, 2004; 145: 2865–75
- Luong QT, O'Kelly J, Braunstein GD et al: Antitumor activity of suberoylanilide hydroxamic acid against thyroid cancer cell lines *in vitro* and *in vivo*. *Clin Cancer Res*, 2006; 12: 5570–77
- Frik M, Fernández-Gallardo J, Gonzalo O et al: Cyclometalated imino-phosphorane gold(III) and platinum(II) complexes. A highly permeable cationic platinum(II) compound with promising anticancer properties. *J Med Chem*, 2015; 58: 5825–41
- Medici S, Peana M, Nurchi VM et al: Noble metals in medicine: Latest advances. *Coord Chem Rev*, 2015; 284: 329–50
- Monroe JD, Hruska HL, Ruggles HK et al: Anti-cancer characteristics and ototoxicity of platinum(II) amine complexes with only one leaving ligand. *PLoS One*, 2018; 13: e0192505
- Chen ZF, Qin QP, Qin JL et al: Water-soluble ruthenium(II) complexes with chiral 4-(2, 3-dihydroxypropyl)-formamide oxoaporphine (FOA): *In vitro* and *in vivo* anticancer activity by stabilization of G-Quadruplex DNA, inhibition of telomerase activity, and induction of tumor cell apoptosis. *J Med Chem*, 2015; 58: 4771–89
- Qin QP, Wang ZF, Huang XL et al: High *in vitro* and *in vivo* tumor-selective novel ruthenium(II) complexes with 3-(2'-Benzimidazolyl)-7-fluoro-coumarin. *ACS Med Chem Lett*, 2019; 10: 936–40
- Wang Y, Pang W, Zeng Q et al: Synthesis and biological evaluation of new berberine derivatives as cancer immunotherapy agents through targeting IDO1. *Eur J Med Chem*, 2018; 143: 1858–68
- Li J, Li J, Jiao Y, Dong C: Spectroscopic analysis and molecular modeling on the interaction of jatrorrhizine with human serum albumin (HSA). *Spectrochim Acta A Mol Biomol Spectrosc*, 2014; 118: 48–54
- Ungerstedt JS, Sowa Y, Xu WS et al: Role of thioredoxin in the response of normal and transformed cells to histone deacetylase inhibitors. *Proc Natl Acad Sci USA*, 2005; 102: 673–78
- Xing M: Molecular pathogenesis and mechanisms of thyroid cancer. *Nat Rev Cancer*, 2013; 13: 184–99
- Lin SF, Huang YY, Lin JD et al: Utility of a PI3K/mTOR inhibitor (NVP-BE235) for thyroid cancer therapy. *PLoS One*, 2012; 7: e46726
- Jin N, Jiang T, Rosen DM et al: Synergistic action of a RAF inhibitor and a dual PI3K/mTOR inhibitor in thyroid cancer. *Clin Cancer Res*, 2011; 17: 6482–89
- Bonner WM, Redon CE, Dickey JS et al: γ H2AX and cancer. *Nat Rev Cancer*, 2008; 8: 957–67
- Stark JM, Pierce AJ, Oh J et al: Genetic steps of mammalian homologous repair with distinct mutagenic consequences. *Mol Cell Biol*, 2004; 24: 9305–16
- Neal JA, Meek K: Choosing the right path: Does DNA-PK help make the decision? *Mutat Res*, 2011; 711: 73–86
- Moynahan ME, Jasin M: Mitotic homologous recombination maintains genomic stability and suppresses tumorigenesis. *Nat Rev Mol Cell Biol*, 2010; 11: 196–207
- Sy SM, Huen MS, Chen J: PALB2 is an integral component of the BRCA complex required for homologous recombination repair. *Proc Natl Acad Sci USA*, 2009; 106: 7155–60
- Ciccia A, Elledge SJ: The DNA damage response: Making it safe to play with knives. *Mol Cell*, 2010; 40: 179–204
- San Filippo J, Sung P, Klein H: Mechanism of eukaryotic homologous recombination. *Annu Rev Biochem*, 2008; 77: 229–57
- Munshi A, Kurland JF, Nishikawa T et al: Histone deacetylase inhibitors radiosensitize human melanoma cells by suppressing DNA repair activity. *Clin Cancer Res*, 2005; 11: 4912–22
- Kotian S, Liyanarachchi S, Zelent A, Parvin JD: Histone deacetylases 9 and 10 are required for homologous recombination. *J Biol Chem*, 2011; 286: 7722–26